Improved Properties of Poly (Methyl Methacrylate) Grafted Polyethylene Glycol for Ocular Prosthetics Applications

Dhaidan Khalaf Kafia[1], Younus K. Jabur[2]

[1]Department of Medical Physics, College of Applied Science, University of Fallujah, Fallujah, Iraq, dhidankhalaf@uofallujah.edu.iq
[2]Renewable Energy Research Center, University of Anbar, Anbar, Iraq

This study aimed to investigate the effectiveness of adding polyethylene glycol (PEG) to poly (methyl methacrylate) (PMMA) for use in ocular prosthetics. Four samples with varying ratios of PEG to PMMA were prepared: 10/90 wt%, 20/80 wt%, 30/70 wt%, and pure PMMA (A). Each sample was characterized using Fourier transform infrared spectroscopy (FTIR), atomic force microscopy (AFM), hardness testing, acid and alkali resistance tests, water absorption testing, wetting angle measurement, and protein deposition assays. The results showed that the addition of PEG improved certain properties such as surface roughness and wetting angle, but also affected other properties like hardness, acid and alkali resistance, and water absorption. Sample C exhibited the lowest surface roughness and wetting angle, while sample A demonstrated the highest hardness and resistance to both acids and alkalis. Sample D showed the least amount of water absorption. Overall, the optimal combination of PEG and PMMA for ocular prosthetics depends on the specific requirements of the intended application.

Keywords: Poly (methyl methacrylate); polyethylene glycol; ocular prosthesis; protein deposits

1. Introduction

Poly(methyl methacrylate) (PMMA), a substance that fits inside the anophthalmic socket and under the eyelids, is typically used to make prosthetic eyes1. They are made to improve facial symmetry, eyelid function, and appearance. The front surface of an artificial eye is similar to that of a contact lens, but while hydrophobic materials have been studied for contact lenses, no study has been done on hydrophilic substance for artificial eye2. These materials could prevent protein deposition and dry eyes on the prosthetic eye surface, which could lessen mucoid discharge and conjunctival inflammatory disease3. A previous study found that prosthetic eyes have been properly polished for vision had greater wettability surfaces than those polished normally, that removing deposits decreased surface wettability and increased conjunctivitis and mucosal problems4. Polyethylene glycol (PEG) is a biocompatible and

environmentally friendly material that has been widely used to graft surfaces and prevent unspecific protein adsorption5. In this study, we synthesized several PMMA/PEG copolymers with Polyethylene glycol as hydrophilic part and PMMA as hydrophobic Original basic. We discussed how the composition of PMMA/PEG influenced its properties for ocular prosthesis applications.

2. Material and methods

The pure samples were prepared according to the ratio 3:2 of polymethyl methacrylate (PMMA) and monomer(MMA). The PEG/PMMA blends were prepared via the solvent casting method as shown Figure 1. First, solutions of PEG and (PMMA with MMA) were separately prepared in beakers, followed by the addition of the PEG solution into the PMMA solution to create a blend. Next, casting samples in templates at room temperature for 14 days resulted in the formation of the final blends. The weight ratio of PEG to PMMA in each blend was adjusted to achieve the desired level of encapsulation without leaking PEG during heating above the

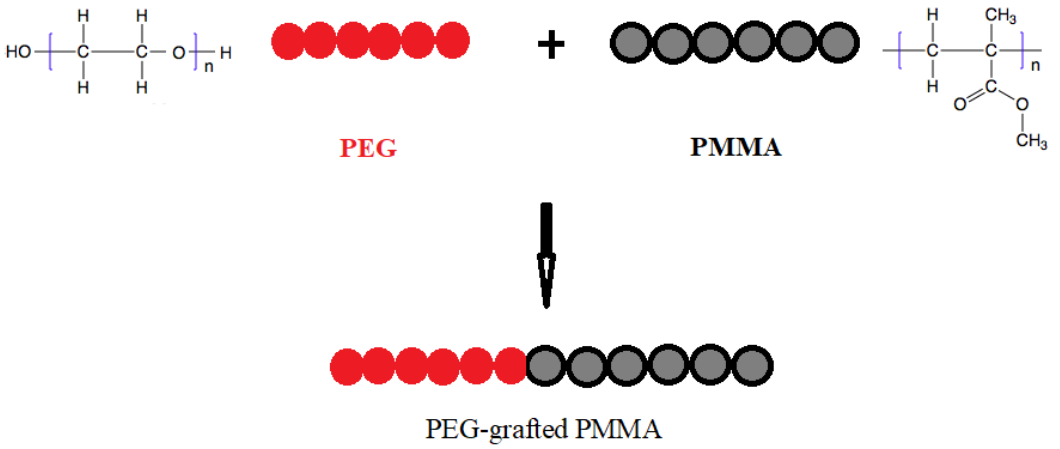

Figure 1. Preparation of the PEG-grafted PMMA method

melting point of PEG. Specifically, three blends were created with the following weight ratios: (a) 10/90% PEG/PMMA; (b) 20/80% PEG/PMMA; and (c) 30/70% PEG/PMMA (Figure 2).

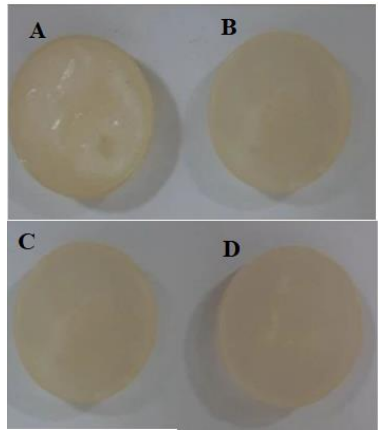

Figure 2. PMMA (A), 10/90 wt % PEG/PMMA (B), 20/80 wt % PEG/PMMA (C) and 30/70 wt % PEG/PMMA (D)

By optimizing the weight ratio of PEG to PMMA, we could maximize the encapsulation efficiency of the blends without compromising their mechanical properties4.

Fourier transform-infrared (FT-IR) spectra were recorded using the KBr technique and a Shimadzu Corporation 8400S FTIR spectrometer. The FT-IR spectrum was measured in the range of 4000–400 cm-1. Atomic force microscopy (AFM) was employed to analyze the surface morphology of PEG-grafted PMMA using an SPM AA-3000 instrument manufactured in the USA.

In this paper, we used a goniometer system with a software-operated camera (Cam 101; KSV Instruments, Bridgeport, CT, USA) to study the dynamics of the wetting process. The system comprises of a pressure chamber, a tilting base, a high-temperature environmental chamber, and an automated droplet dispensing unit. The droplet spreading behavior and contact angle are photographed using a high-speed camera system. Because external vibrations might lead to measurement mistakes, the goniometer is mounted to a robust table to minimize interference. The measurements were carried out in air that was sufficiently free of dust and organic vapors. The surface characteristics of the sample or the probe droplet may change as a result of organic vapors adhering to them. The measurements may also be negatively impacted by airborne dust that adheres to the sample or the water. A tissue soaked in 70% ethanol was used to wipe off PMMA sample disks with low, normal, and high surface polishes to remove contamination, permitted to dry, then set up in the goniometer.

To calculate the samples' percentage weight increase after 24 hours in the water, we followed the standard test method for water absorption of plastics as set forth by ASTM D570 - 98. This method involves measuring the mass of the sample before and after exposure to water, and calculating the difference between the two values as a percentage of the initial weight6.

Shore Durometer D Elcometer 3120 was used to measure the hardness of thermally hardened polymeric materials and Gesan Chem 100 Semi-Automatic Biochemistry Analyzer was used.

Method of deposition protein measurement.

Proteins are a key component in body fluids and adhere to most biomaterials within seconds

of their exposure . There have been numerous studies of lipid and/or protein deposition on contact lens materials but no investigations of deposits on prosthetic eye material appear to have been carried out 7. To measure the total protein for each sample, 100 milligrams of protein was added to 100 milliliters of distilled water in a container and the protein was dissolved in water and this is the standard solution. The samples are immersed in the solution for hours or minutes. After this time, each of the samples is washed separately with the minimum amount of distilled water. Four samples are obtained from the water that is specific to each sample. Then we put the water of each sample in a test tube to measure its total protein. 1000 microliters of total protein was placed in 5 test tubes .After that, it is added to the four water tubes for each sample and the total protein in the fifth tube is added to the standard solution before immersing the samples, then the tubes are shaken and left for 5 minutes. Then it is placed in a biochemistry analyzer, and then we get the results

3. Results and discussion

3.1. FTIR analysis

FTIR spectroscopy was used to investigate the interactions between PMMA and PEG in the blends and different PMMA/PEG ratios. Spectra were collected in the 4000–400 cm−1 range and are presented in Figure 3. The Poly MMA showed distinctive peaks at 2980 cm−1 and 2900 cm−1, which were attributed to C-H asymmetric stretching in CH3 and CH2, respectively. The C-H symmetric stretching in CH3 was responsible for the peak at 2832 cm−17,8. The ester carbonyl stretching vibration (C=O), which is the typical peak for neat PMMA, was observed at 1741 cm−17,8. Additional peaks were observed at 1490 cm−1 and 1431 cm−1, attributed to CH3 deformation modes. The ester bond (C–O–C) stretching vibration was detected at 1109 cm−1. The bond (C–C) stretching peak showed at 930 cm−19. Finally, the high peaks at 848 cm−1 and 711 cm−1 were associated with CH2 bending and C=O bending , respectively10. In the PEG-grafted PMMA, the C-H stretching peaks were found at similar wave numbers compared to those in pure PMMA. The carbonyl peak position in the blend was comparable to that in PMMA, yet its shape was narrower. The O-H stretching peaks at approximately 3797 cm−1 widened in the blend, possibly due to the carbonyl–hydroxyl interaction. These findings supported the conclusion reached by Sari et al.11, who reported the formation of a new compound through the combination of PMMA and PEG. However, the phase transformation process is influenced not only by the fundamental chemical structure of a polymer but also by various internal and external factors.

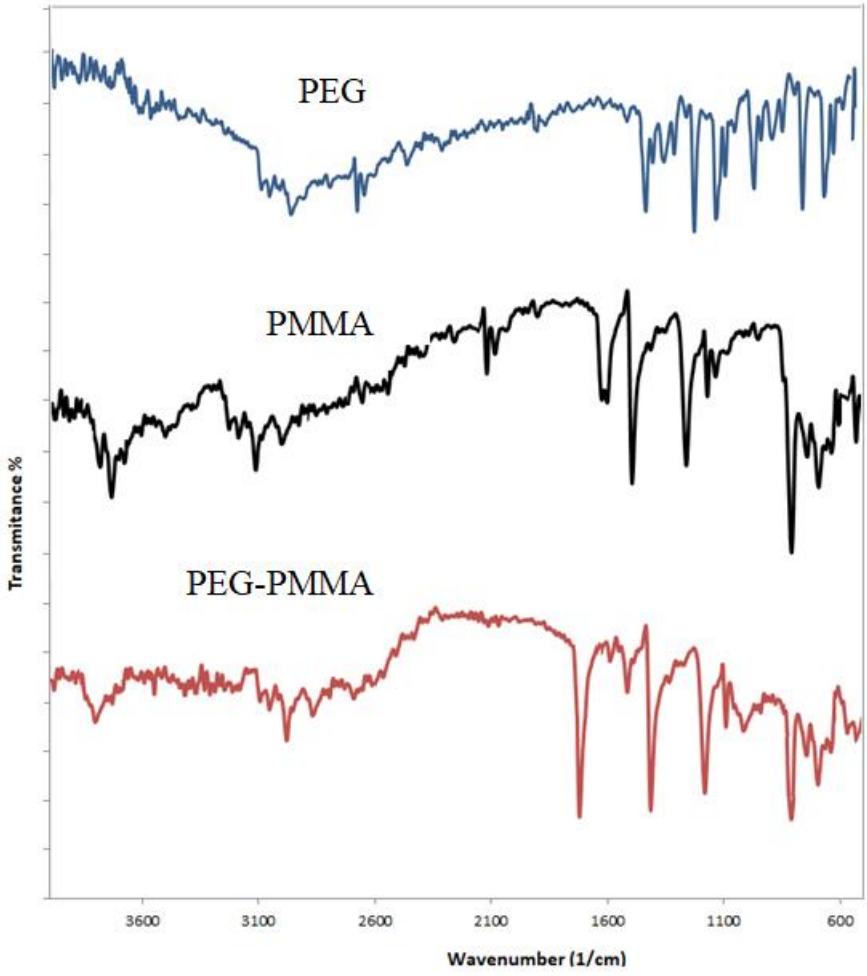

Figure 3. FTIR spectra of PEG, PMMA, and PEG/PMMA blend

3.2. The surface morphology of the samples by AFM

The surface morphology of the samples affects their properties, which are important for applications such as adhesion. The surface roughness of the sample is one of the factors that influences the adhesion properties. A higher surface roughness leads to a higher adhesion. Therefore, it is crucial to analyze the surface morphology of the pattern. The surface morphology of the PMMA changed into measured via AFM and is shown in Figure 4. The results demonstrate that the surface roughness (RMS) of samples A, B, C, and D are 34.5 nm, 21.54 nm, 11.57 nm, and 16.2 nm, respectively. The outcomes suggest that the RMS roughness decreases with increasing the awareness of the PEG-grafted PMMA within the solution. It can be seen that the higher percentage of concentration of PEG-grafted PMMA reduces the surface roughness of the PMMA. A good agreement with the results of preceding studies1,12 [1, 14] was observed. However, the increase in this concentration influences the other features of materials. The use of optimization of the polishing parameters could improve the relation between the polishing step and root mean square (RMS). By managing the polishing

conditions, such as the polishing time and pressure, the surface roughness may be reduced, resulting in a better compatibility among the mating parts13.

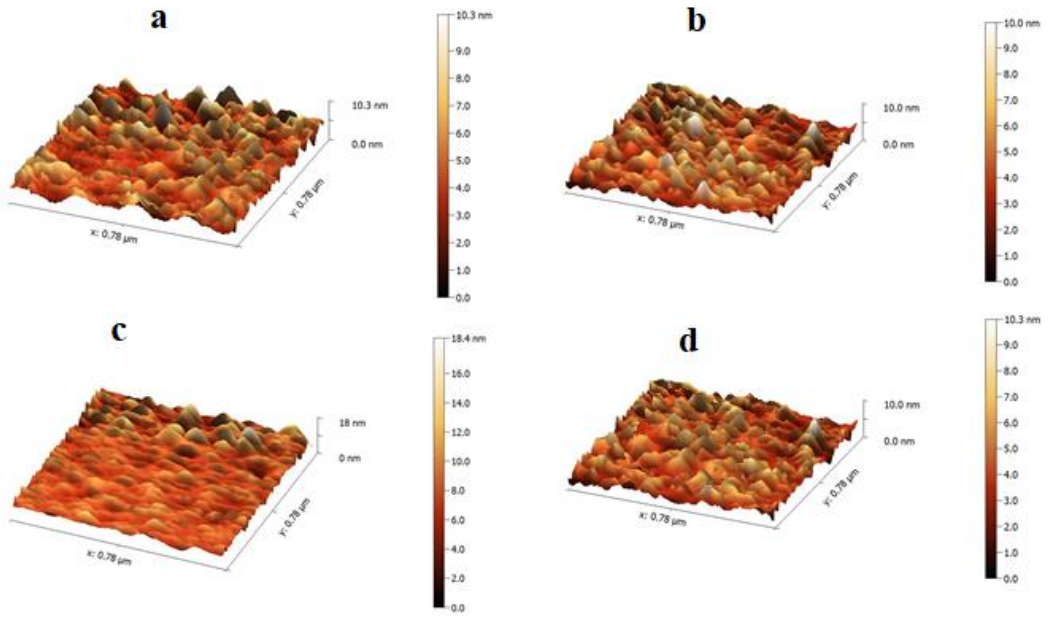

Figure 4. AFM images for samples: PMMA (a), 10/90 wt % PEG/PMMA (b), 20/80 wt % PEG/PMMA (c) and 30/70 wt % PEG/PMMA (d)

3.3. Wetting angles of PMMA with different PEG

The wetting angles for the several of PEG/PMMA blends are shown in Figure 5. The following wetting angles were measured for the samples: Sample (A) 76º, Sample (B) 79.9º, Sample (C) 46º, and Sample (D) 42º. An inverse relationship is observed between the wetting angle and the amount of different PEG/PMMA blends. This means that the wetting angle is reduced and the water adhesion is increased as the percentage of PEG is increased. This result is in agreement with previous research. The water adhesion to the material is increased by this, which helps moisturize the eye, prevents it from drying out and reduces the adhesion of sediments such as proteins. It is convenient if the material is used in the manufacture of artificial eyes 4,14. However, an appropriate amount must be used, such as the proportion in sample C (20/80 wt % PEG/PMMA)12.

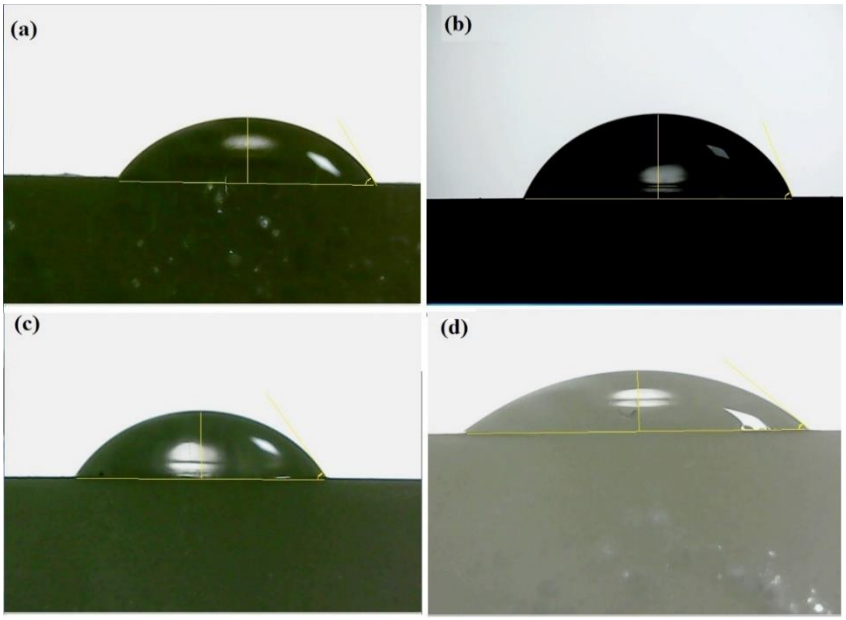

Figure 5. The wetting angle: (a) PMMA, (b) 10/90 wt % PEG/PMMA, (c) 20/80 wt % PEG/PMMA and (d) 30/70 wt % PEG/PMMA

3.4. Acid and alkali test

The polymeric membrane is weighed in its dry form, and then immersed in different buffer solutions of pH 2, 4, 6, 8, and 10 for 24 hours. After that, the membrane is rinsed with distilled water for 3 minutes to remove any traces of the solutions, and then dried thoroughly. The weight of the membrane after drying is recorded, and the weight difference between the dry and treated membrane is calculated. The solution that causes a loss of membrane weight is identified, and from it the pH range that the membrane can operate without damaging its structure is determined.

The acid test (pH) results for the samples are presented in Table 1. This experiment determined the weight difference between the samples' initial and final weights in the solution. The findings revealed that all samples' weight differences were quite small, demonstrating that the samples were resistant to acid degradation. Sample C (20/80 wt% PEG/PMMA) had the greatest weight difference between the samples, while Sample A (pure PMMA) had the smallest weight difference. This outcome is in line with the features of the ocular prosthesis, which must be extremely durable and stable in acidic environments ambiances15,16.

Table 1. The results of the acid test

pH	Sample A (g)	Sample B (g)	Sample C (g)	Sample D (g)
2	0.02	0.02	0.01	0.02
4	0.03	0.02	0.021	0.03
6	0.02	0.05	0.08	0.06
8	0.02	0.03	0.02	0.01
10	0.025	0.02	0.03	0.02

3.5. Water absorption test

The climatic chamber is set to a temperature of 30°C and a relative humidity of 50%. The samples to be tested have equal dimensions and are immersed in tap water with a depth of 25 mm for 10 minutes. Then, the samples are placed on a metal net to drain the excess water for another 10 minutes. The water droplets on the tip of the samples are removed using blotting paper. The weight of the samples is measured and expressed as a percentage of their initial weight.

Table 2 presents the results of the water absorption test for the ocular prostheses. As shown in the Table 2, the weight of the pure sample after immersion was 0.012 grams. The second sample had an increase of 0.015 grams, while the third sample showed an increase of 0.024 grams. The fourth sample had the smallest increase, at 0.02 grams. These results indicate that the third sample had the highest level of water absorption, followed by the second and fourth samples, respectively. The first sample had the least amount of water absorption, which is consistent with the properties of the ocular prosthetic device and the findings reported in Reference 17.

Table 2. Results of water absorption test

Sample	Weight before water immersion (g)	Weight after water immersion (g)
(A) PMMA	8.31	8.322
(B) 10/90 wt % PEG/PMMA	8.88	8.895
(C) 20/80 wt % PEG/PMMA	8.11	8.134
(D) 30/70 wt % PEG/PMMA	8.49	8.51

3.6. Hardness test

The hardness of the sample was measured using a Shore durometer, which is a device that measures the resistance of thermally hardened polymer materials to indentation by a needle. The device has a circular dial with a needle in the center. The sample was placed on a designated area and pressed against the needle, which penetrated the sample and gave a reading of its hardness after about 30 seconds. This procedure was repeated six times on both sides of the sample, and the average of all readings was taken as the hardness value of the sample.

Figure 6 shows the results of the hardness test, where the values were measured in kgf/mm². The first sample (A) yielded the highest result of 81 kgf/mm², while the sample D produced the lowest result of 59 kgf/mm². These results correspond to the expected properties of the ocular prosthesis18,19.

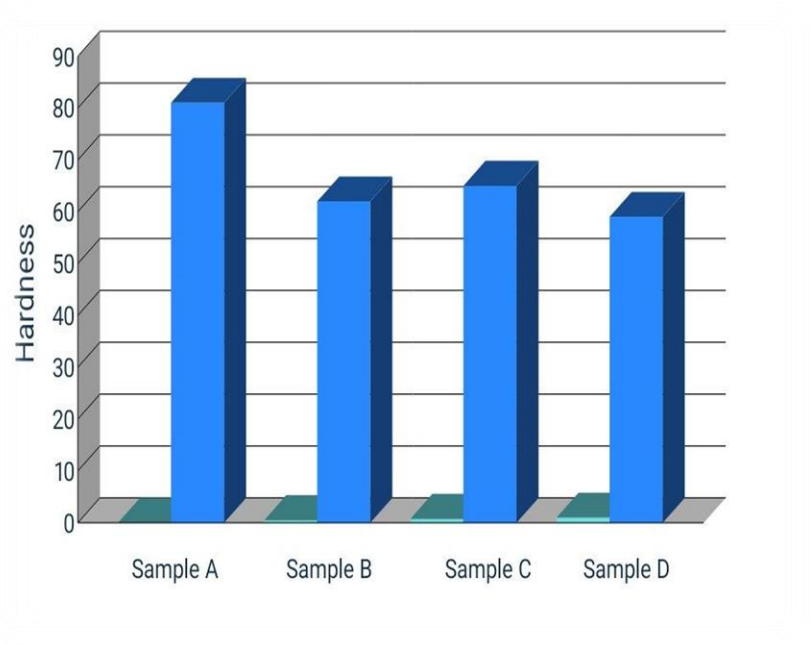

Figure 6. The relationship between samples and hardness. (A) PMMA, (B) 10/90 wt % PEG/PMMA, (C) 20/80 wt % PEG/PMMA and (D) 30/70 wt % PEG/PMMA

3.7. Rates of deposition protein on PMMA samples

Previous studies have focused on the deposition of lipids and/or proteins on contact lens materials, but no research has been done on the deposits on prosthetic eye materials. The amount to protein removed from the face of PMMA and PEG/PMMA samples after incubation in a protein-rich artificial solution was measured20. The results showed that there was a large dissimilarity in the quantity of protein between PMMA and PEG/PMMA for all incubation times (6, 12, and 24 hours). The 10/90 wt % PEG/PMMA samples had significantly less protein than PMMA, while the 20/80 wt % and 30/70 wt % PEG/PMMA samples had similar amounts of protein as PMMA. The total protein extracted from PMMA did not increase over the 1 day of incubation, while the PEG/PMMA samples showed a slight increase. The data are summarized in Table 3.

Table 3. Sum protein removed from the surface deposits of PMMA for different time in protein/lipid ATS

Polishing	Inside the protein (hours)	Result g/dl
PMMA	6	1.1778
10/90 wt % PEG/PMMA	6	1.0003
20/80 wt % PEG/PMMA	6	1.1501
30/70 wt % PEG/PMMA	6	1.0461
PMMA	12	1.1547
10/90 wt % PEG/PMMA	12	1.0325
20/80 wt % PEG/PMMA	12	1.1550

30/70 wt % PEG/PMMA	12	1.1731
PMMA	24	1.1781
10/90 wt % PEG/PMMA	24	1.0648
20/80 wt % PEG/PMMA	24	1.1517
30/70 wt % PEG/PMMA	24	1.1517

The amount of protein removed from the samples after incubation in a protein-rich solution for different time periods is shown in the Table 3. The samples were divided into three groups: the first group was incubated for 6 hours, the second group for 12 hours, and the third group for 24 hours. The samples were incubated by the researchers. The amount of protein on the samples was increased with the incubation time by the protein-rich solution, except for the third group, which showed a constant value. This was suggested by the results. The samples were reached a saturation point after 24 hours, where no more protein could adhere to them by the protein-rich solution. The possible explanations for this phenomenon were that the protein particles were either detached from the samples due to long exposure, or a stable layer was formed by them that prevented further adsorption21-23.

4. Conclusions

Our novel study investigates the effects of adding PEG at different concentrations to the prosthetic eye material. The findings illustrate that PEG has various effects on the properties of the material, which includes hardness, water absorption, acid and alkali resistance, wetting angle and protein deposition. The following points summarize the principle findings:

- The pure PMMA sample (A) had the first-rate overall performance in the hardness and the acid and alkali tests, indicating that PEG did not enhance the mechanical and chemical stability of the material.

- The 10/90 wt % PEG/PMMA sample (B) had the optimal performance including the below tests: water absorption, the protein deposition, and the wetting angle, indicating that PEG improved the hydrophilicity and biocompatibility of the material. This means that PEG moisturized the eye, avoided dry eyes, reduced protein accumulation that could motive inflammation, and enhanced the wettability of the material.

- The 20/80 wt % and 30/70 wt % PEG/PMMA samples (C and D) exhibit no considerable improvement in any current tests compared to PMMA.

This work provides useful insights into how surface wettability and Protein deposition on PMMA materials are impacted via varying surface finishes and addition PEG. These factors are vital for the interpalpebral surface of the prosthesis, in which they could make the eyelids' normal motion and the washing impact of tears simpler. Additionally, they assist tears lubricate the prosthesis whilst it's first positioned in the socket and earlier than tear protein deposits shape. The addition of PEG had a positive impact in a few tests and progressed ocular prosthesis material.

References

1. Ko J, Cho K, Han SW, Sung HK, Baek SW, Koh W-G, et al. Hydrophilic surface modification of poly (methyl methacrylate)-based ocular prostheses using poly (ethylene glycol) grafting. Colloids and Surfaces B: Biointerfaces. 2017;158:287-94.
2. Luensmann D, Jones L. Albumin adsorption to contact lens materials: A review. Contact Lens and Anterior Eye. 2008;31(4):179-87.
3. Pine KR, Sloan B, Jacobs RJ. Deposit buildup on prosthetic eyes and implications for conjunctival inflammation and mucoid discharge. Clinical Ophthalmology. 2012:1755-62.
4. Pine KR, De Silva K, Zhang F, Yeoman J, Jacobs R. Towards improving the biocompatibility of prosthetic eyes. Heliyon. 2021;7(2):e06234.
5. Chen H, Yuan L, Song W, Wu Z, Li D. Biocompatible polymer materials: role of protein-surface interactions. Progress in Polymer Science. 2008;33(11):1059-87.
6. Gould TE, Piland SG, Shin J, Hoyle CE, Nazarenko S. Characterization of mouthguard materials: Physical and mechanical properties of commercialized products. Dental materials. 2009;25(6):771-80.
7. Luensmann, Doerte, and Lyndon Jones. "Protein deposition on contact lenses: the past, the present, and the future." Contact Lens and Anterior Eye 35.2 (2012): 53-64.
8. Hayat MD, Zhang H, Karumbaiah KM, Singh H, Xu Y, Zou L, et al. A novel PEG/PMMA based binder composition for void-free metal injection moulding of Ti components. Powder Technology. 2021;382:431-40.
9. Coiai S, Prevosto D, Bertoldo M, Conzatti L, Causin V, Pinzino C, et al. Chemistry of interfacial interactions in a LDPE-based nanocomposite and their effect on the nanoscale hybrid assembling. Macromolecules. 2013;46(4):1563-72.
10. Bokovets SP, Pertsevoi FV, Murlykina NV, Smetanska IM, Borankulova AS, Ianchyk MV, et al. Investigation of infrared spectra of agar-based gel systems for the production of jelly bars. Journal of Chemistry and Technologies. 2023;31(1):92-103.
11. Hadjiivanov KI, Panayotov DA, Mihaylov MY, Ivanova EZ, Chakarova KK, Andonova SM, et al. Power of infrared and raman spectroscopies to characterize metal-organic frameworks and investigate their interaction with guest molecules. Chemical Reviews. 2020;121(3):1286-424.
12. Sari A, Alkan C, Karaipekli A, Uzun O. Poly(ethylene glycol)/poly(methyl methacrylate) blends as novel form-stable phase-change materials for thermal energy storage. Journal of Applied Polymer Science. 2009;116:929-33.
13. Suzuki Y, Onozato S, Shinagawa Y, Matsumoto A. Microporous structure formation of poly (methyl methacrylate) via polymerization-induced phase separation in the presence of poly (ethylene glycol). ACS Omega. 2022;7(43):38933-41.
14. Zhang W, Zhang X. Study on surface structure and properties of PMMA/PEG copolymer coatings. Materials Research Innovations. 2014;18:S2-1028.
15. Bi H, Meng S, Li Y, Guo K, Chen Y, Kong J, et al. Deposition of PEG onto PMMA microchannel surface to minimize nonspecific adsorption. Lab on a Chip. 2006;6(6):769-75.
16. Kambala SS, Rathi D, Borle A, Rajanikanth K, Jaiswal T, Dhamande M. Evaluating the color stability of ocular prosthesis after immersion in three different immersion media: An in vitro study. Journal of International Society of Preventive & Community Dentistry. 2020;10(2):226.
17. Da Costa GC, Aras MA, Chalakkal P, Da Costa MC. Ocular prosthesis incorporating IPS e-max press scleral veneer and a literature review on non-integrated ocular prosthesis. International Journal of Ophthalmology. 2017;10(1):148.
18. Goiato MC, dos Santos DM, Moreno A, Iyda MG, Rezende MCRA, Haddad MF. Effect of disinfection and storage on the flexural strength of ocular prosthetic acrylic resins. Gerodontology. 2012;29(2):e838-e44.

19. Abd Kati F, Al-Kaabi AFJ. Effect of oil paint addition on micro hardness of acrylic ocular prosthesis. Iraqi Dental Journal. 2016;38(2):87-9.
20. Dos Santos DM, Nagay BE, da Silva EVF, da Rocha Bonatto L, Sonego MV, Moreno A, et al. In vitro analysis of different properties of acrylic resins for ocular prosthesis submitted to accelerated aging with or without photopolymerized glaze. Materials Science and Engineering: C. 2016;69:995-1003.
21. De Geyter N, Morent R, Van Vlierberghe S, Dubruel P, Leys C, Gengembre L, et al. Deposition of polymethyl methacrylate on polypropylene substrates using an atmospheric pressure dielectric barrier discharge. Progress in Organic Coatings. 2009;64(2):230-7.
22. Hlady V, Buijs J, Jennissen HP. [26] Methods for studying protein adsorption. In: Wetzel R, editor. Methods in Enzymology. 309. Amsterdam: Elsevier; 1999. p. 402-29.
23. Contado C, Mehn D, Gilliland D, Calzolai L. Characterization methods for studying protein adsorption on nano-polystyrene beads. Journal of Chromatography A. 2019;1606:460383.
24. Schmidt DR, Waldeck H, Kao WJ. Protein adsorption to biomaterials. In: Puleo D, Bizios R, editors. Biological interactions on materials surfaces. New York: Springer; 2009. p. 1-18.